TÜBİTAK

Research Article

Transient- and probabilistic neural network-based fault classification in EHV three-terminal lines

Ravi Kumar Varma BHUPATIRAJU*, **Venkata Sesha Samba Siva Sarma DHANIKONDA,**
Venkata Ramana Rao PULIPAKA
Department of Electrical Engineering, National Institute of Technology, Warangal, India

Abstract: This paper presents a fast and accurate fault classifier for three-terminal transmission circuits. Traditional phasor-based methods fail to meet the high speed requirements of modern power grids and necessitate alternative solutions. The transient-based schemes use advanced signal processing techniques to achieve fast and accurate fault classification. As the three-terminal lines experience very pronounced transients during faults, the proposed method makes use of the fault-generated transients to quickly and correctly classify the fault. Many transient-based schemes fail to give the required accuracy since the transient patterns with relay-measured signals are highly influenced by fault conditions. Therefore, a thorough analysis of transient patterns is carried out in this paper, and based on the typical patterns revealed by the analysis of fault-generated transients an effective classification algorithm is developed. For high-speed classification, only a quarter-cycle of postfault voltage signals measured at the relay points will be processed for feature extraction using wavelet transform. The algorithm includes a hybrid procedure based on a probabilistic neural network for tackling the effects of fault inception angle and fault resistance in transient variations. Particularly, it is designed to overcome the problem with double-line-to-ground fault classification. The technique is simple and extensive simulation studies and comparison substantiate the efficacy of the proposed method under different fault conditions.

Key words: Three-terminal lines, fault classification, transients, wavelet transform, probabilistic neural network

1. Introduction

Modern power grids are becoming complex interconnected power systems to facilitate the optimal utilization of existing infrastructure and resources. In such power systems, extra-high voltage transmission lines carry the bulk of the power to meet the demand at different load centers. Transmission lines play a vital role in maintaining the grid integrity and therefore must have very effective protective relays for the reliable and stable operation of the grid. Generally, a three-terminal line configuration is created if construction of a new substation is not possible due to cost or right-of-way concerns. Significantly, due to lack of measurements at the tap point, a three-terminal line protection requires further enhancements [1]. Figure 1 shows such a 400 KV line structure present in an Indian power grid [2].

In transmission line protection, after fault detection, the line relay invokes a fault classification function to identify the type of fault and the faulted phases for initiating possible single-pole tripping and autoreclosing [3]. Hence, the fault classifier must be very quick and accurate to maintain system stability and continuity of supply. Many fault classification algorithms are traditionally phasor-based, where the estimation of postfault

---

*Correspondence: bhrkvarma@yahoo.co.in
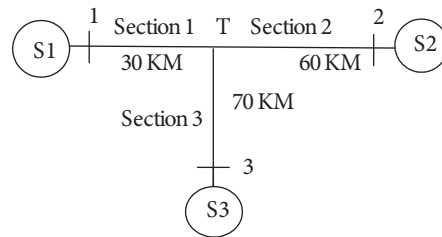
Figure 1. A 400 KV three-terminal transmission circuit.

voltage/current phasors requires at least a half-cycle of data. Most of these methods are affected by dynamically changing network configuration and fault conditions. Recently, a phasor-based method using sequential reactive powers was proposed by Mahamedi and Zhu [4]. Despite its claim to be setting- and synchronization-free, one entire cycle of fault data requirement is a critical factor influencing the speed of response.

Driven by the need for high-speed relaying, with the availability of efficient signal-processing techniques and high-sampling-rate hardware a new class of classification algorithms based on fault-induced transients has evolved. These transient-based algorithms process fault-generated traveling waves or high-frequency components for feature extraction, mostly by using wavelet transform. In [5], a method using an initial current traveling wave is reported, mentioning that it fails during three certain phase faults. A wavelet singular entropy-based technique is presented in [6] by using a half-cycle postfault voltage signal. The problem with this method is it requires the setting of three thresholds according to system situation. Another current transient-based classification technique is proposed in [7], whose accuracy with double-line to ground (LLG) faults is only around 90%. Despite their speed advantage, a major problem for all these deterministic transient-based methods is the influence of fault inception angle (FIA) and fault resistance (R_f) on the fault transient magnitudes. Particularly, LLG fault classification poses a big challenge due to misleading transient patterns generated during the faults.

In an effort to overcome the above problems due to system inconstancy and for better performance, several authors explored artificial intelligence applications with fuzzy logic [8,9], artificial neural networks (ANNs) [10,11], support vector machines (SVMs) [12,13], etc., to solve the fault classification problem. The inputs to these knowledge-based methods are mainly either steady-state or transient components of the fault voltage/current signals. Recently, Jamehbozorg and Shahrtash proposed a decision tree (DT)-based method with half-cycle discrete Fourier transformation (HCDFT) [14], which requires computation of ten odd harmonic phasors. A statistical DT-based approach [15] is accurate, but it takes two full cycles of current signals for transient extraction. Another transient-ANN approach was developed with a rough membership neural network in [16], but the results presented include only a 90° variation of FIA. In addition to all the above methods primarily developed for two-terminal lines, a transient SVM-based classifier is designed for three terminal lines in [17]. However, its poor performance (95% accuracy) in classifying grounded faults is not acceptable. In view of the above drawbacks, a thorough investigation into the transient patterns generated during faults is necessary for developing a useful classifier.

In this paper, a new transient-based scheme for fast and accurate fault classification is proposed for three-terminal lines. The proposed algorithm extracts the distinguishing features from the three phase voltage signals by using wavelet transformation and a probabilistic neural network (PNN) is included to improve the accuracy of the classifier with LLG faults. Unlike many other techniques, the scheme is simple, requires single threshold setting, and its speed and accuracy are significantly high. The performance of the method is verified by simulation of a three terminal line shown in Figure 1 using MATLAB/SIMULINK environment.

In Section 2, the feature extraction is described, followed by feature analysis and algorithm formulation. Section 3 presents the simulation details and performance results of the proposed algorithm. Finally, conclusions are given in Section 4.

2. Transient features and algorithm formulation

Fault classification methods process voltage signals and/or current signals measured by the relays to extract necessary discriminating features. Since most of the available algorithms use only postfault signals, the size of a signal window plays an important role in deciding the speed and accuracy of the classification procedure. A larger window size normally improves accuracy at the cost of speed and vice versa. However, use of a smaller window without losing much accuracy is possible in transient-based schemes because of the wide-band nature of the fault transients. In the proposed method, only postfault voltage signals of a quarter cycle duration from all the three ends are taken as inputs and the choice is based on the fact that voltage transients are more than current transients during faults in power systems [18]. A sampling frequency of 200 kHz is used as the faulted lines contain high frequency components in the range of 10–100 kHz [19]. Such a sampling rate is common with currently available hardware and, in addition, avoids the use of an antialiasing filter in digital relays [20]. The high-frequency components present in voltage signals are extracted by using discrete wavelet transform (DWT), which has proven to be an effective signal processing tool for power systems [21].

The feature extraction procedure is presented below, followed by a discussion on fault transient patterns for developing the classification procedure.

2.1. Feature extraction

Figure 2 depicts the overall structure of the proposed scheme in which the classifier is activated by the fault detector when a fault is detected in the line. The classifier algorithm takes the three phase voltage signals (V_a, V_b, and V_c) of 1/4 cycle time from the three ends and forms the line voltages (V_{ab}, V_{bc}, V_{ca}) and zero-sequence voltage (V_0) from the phase voltages. In spite of the communication requirements, use of three end signals improves the feature strength, as explained later. The quarter-cycle windows of all fault voltage signals shown in Table 1 are then decomposed to the first level by using the multiresolution analysis feature of the DWT.
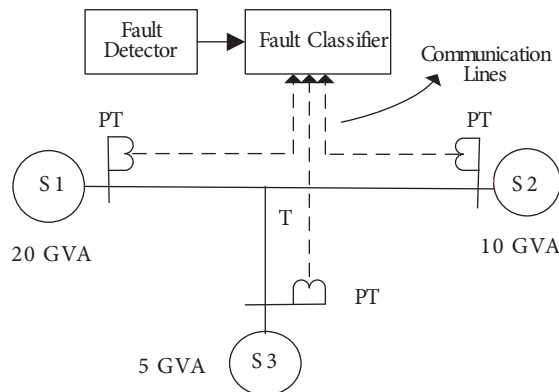
Figure 2. Signal communication for the proposed fault classifier.

Table 1. Voltages decomposed by the DWT.

End	Phase voltages	Line voltages	Zero sequence voltages
1	V_{a1}, V_{b1}, V_{c1}	V_{ab1},V_{bc1},V_{ca1}	$V_{01} = (V_{a1} + V_{b1} + V_{c1})/3$
2	V_{a2}, V_{b2}, V_{c2}	V_{ab2},V_{bc2},V_{ca2}	$V_{02} = (V_{a2} + V_{b2} + V_{c2})/3$
3	V_{a3}, V_{b3}, V_{c3}	V_{ab3},V_{bc3},V_{ca3}	$V_{03} = (V_{a3} + V_{b3} + V_{c3})/3$

The DWT of a digital signal is given by

$$DWT(m,k) = \frac{1}{\sqrt{a_0^m}} \sum_n x(n)g\left(\frac{k - nb_0 a_0^m}{a_0^m}\right),$$

(1)

where $g(n)$ is the mother wavelet and $x(n)$ is the input signal, and the scaling and translation parameters a and b are functions of integer parameter m. Figure 3 shows measured phase voltage signals at end-1 for an AG fault with the fault inception at 0.025 s. A 5 ms postfault voltage signal window and the first-level detail coefficients (D1) coefficients of phase and zero-sequence voltages obtained using wavelet transformation are also indicated.

Although many earlier techniques used higher-level decomposition, in this paper only first-level is preferred due to computational simplicity and accuracy of transient energy calculation. The transient-based meth-
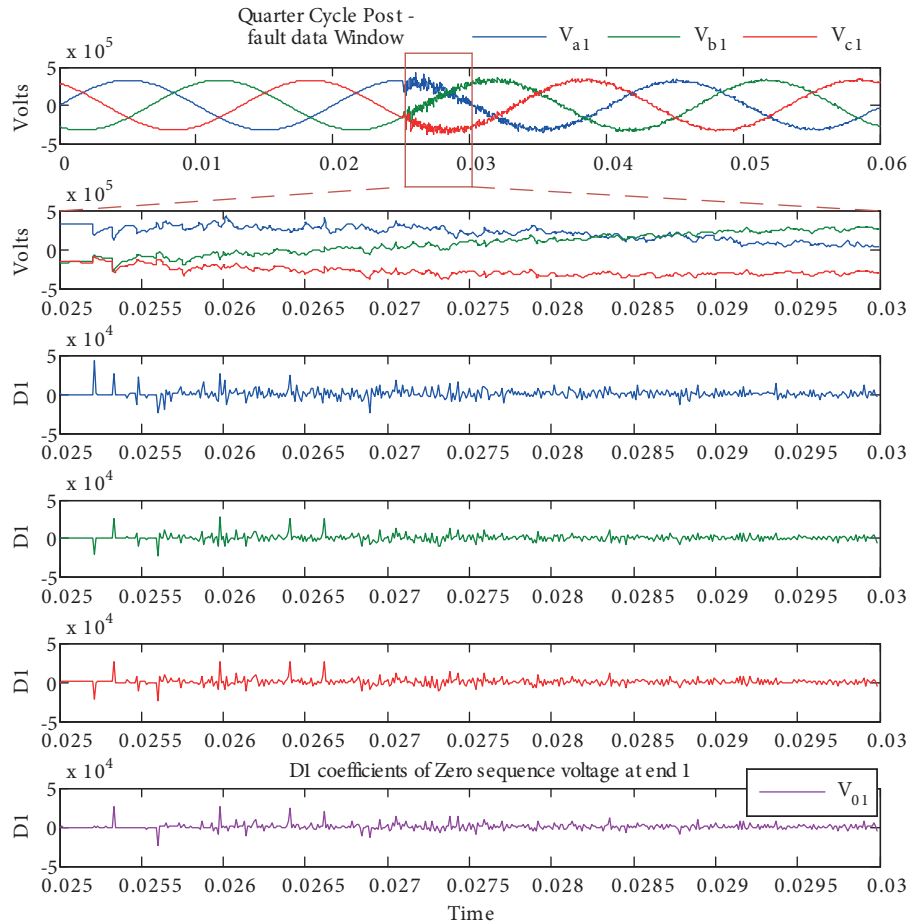
Figure 3. Phase voltages at end 1 and the D1 coefficients with an AG fault in Section 3.

ods need denoising of input signals before their processing to avoid the effect of noise and an assumption is made to that effect with the proposed method in this paper.

From the D1 coefficients, the transient signal energy for each voltage signal is calculated by using the equation

$$\text{Transient energy } \psi = \sqrt{\sum_{i=1}^{N}\left[D1\left(i\right)\right]^{2}}, \tag{2}$$

where N is the number of first-level detail coefficients after truncation of five samples, applied to eliminate the edge effect.

Now the effective transient energy for each voltage signal is obtained by adding the signal energies of the three ends (1, 2, and 3). The effective transient energy for phase, line, and zero-sequence voltage signals is given by

$$\Psi_{i} = \Psi_{i1} + \Psi_{i2} + \Psi_{i3} \;; i = abc$$

$$\Psi_{jk} = \Psi_{jk1} + \Psi_{jk2} + \Psi_{jk3} \;; j = abc \,\&\, k = bca$$

$$\Psi_{0} = \Psi_{01} + \Psi_{02} + \Psi_{03},$$

where Ψ_{i} is the effective transient energies of phase voltages, Ψ_{jk} is the effective transient energies of line voltages, and Ψ_{0} is the effective transient energy of the zero-sequence voltage. The above set of energies is normalized to form a feature array, called the normalized effective transient energy (NETE) array, as shown in Figure 4. The NETE array, describing the high-frequency transient content on voltage signals, is used as input for classifying faults in the present technique.
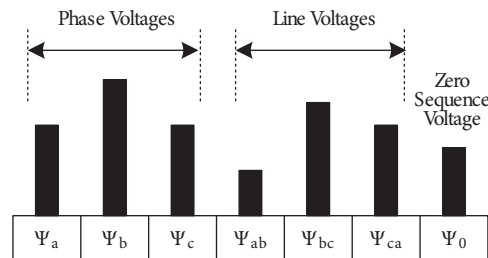
Figure 4. NETE array input to the classifier.

In the above procedure, the addition of three end energies is done to improve the sensitivity of the scheme with respect to the fault location and R_{f}. In close-up faults, the voltage signal of the faulted phase measured by the relay (at the faulted section end) contains very little transient energy. However, the relays at the other two ends find appreciable energy in the measured signals. Therefore, use of only single-end measurements leads to errors in classification of close-up faults.

2.2. Analysis of transient patterns:

Many transient-based classification techniques depend on a comparison of the fault transient energy magnitudes of different phase voltages or currents and these magnitudes widely vary depending on the type of fault and fault parameters. Therefore, methods based on the direct energy threshold fail to give accuracy and normalization becomes a necessity to fix the thresholds. Despite the normalization, threshold fixing is difficult and often leads

to inaccurate classification. An advantage of the proposed method in this paper is that it requires a single threshold fixing.

The NETE feature array formed from the fault voltage signals will provide the necessary information for classifying the fault. Initially, the ground involvement in the fault can be checked by verifying the energy on zero sequence voltages, i.e. Ψ_0. For ungrounded faults, its value will be zero.

2.2.1. Grounded faults

Single line-to-ground (LG) faults: In LG faults, which amount to 85% of total faults in power systems, the unfaulted phases also contain energy magnitudes that are close to that of the faulted phase. The unfaulted phase energies (Ψ_b and Ψ_c) are nearer to the faulted phase energy (Ψ_a), thus making segregation of the faulted phase difficult. Instead of using phase voltage energies, the proposed method uses energy on line voltages to resolve this problem. Observing the energy on line voltages, Ψ_{bc} becomes zero, clearly indicating that the fault is on phase A. Similarly, Ψ_{ca} and Ψ_{ab} will become zero for BG and CG faults, respectively.

LLG faults: Accuracy of classification in many algorithms is mainly affected by LLG faults, which create misleading energy patterns. Although in many situations the faulted phases carry higher magnitudes of transients than the unfaulted phases, during certain ranges of FIA, depending on the R_f, the transient presence occurs the other way. Further, Figure 5 demonstrates the variation in energy with respect to FIA on phase voltages during a BCG fault. The energy on faulted phases is more than the unfaulted for many inception angles, except in the band from 60 to 130°. The width of this band is again a function of the R_f. Similar inconsistent patterns appear for ABG and CAG faults, also with error bands between 0 and 180°. Nearly 1/3 of the LLG faults will be misclassified if the decision is based on the comparison of energy present on individual phases. Hence, a neural network is considered a preferable solution for LLG fault classification in this work.
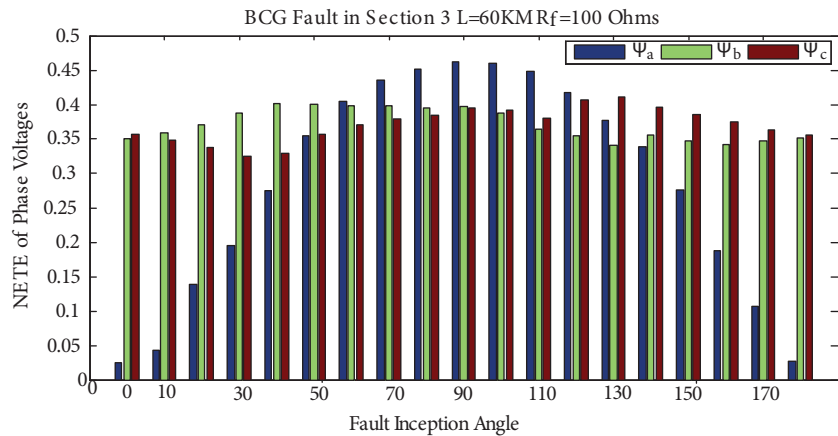

Figure 5. Variation of energy on phase voltages with FIA (BCG fault).

2.2.2. Ungrounded faults

In the case of line-to-line (LL) faults, the two faulted phases contain equal values of transient energy in their phase voltages and the other phase contains no transient energy. This distinctive feature clearly segregates an LL fault and the ground is not involved in the fault. If the above condition is not satisfied during a fault without ground involvement, then the fault is decided to be a three-phase (LLL) fault.

2.3. Algorithm formulation

Based on the above feature analysis, a hybrid algorithm is developed in this paper to classify all types of faults very accurately. In this algorithm, determination of ground involvement and classification of LG, LL, and LLL faults will be carried out by a deterministic procedure, as explained earlier. For LLG faults, in view of the misleading transient patterns, a neural network is incorporated, thus making the algorithm a hybrid one. The algorithm takes the NETE array as input and initially checks whether the fault is grounded or not. If the fault does not involve the ground, then it checks for LL or LLL faults. In the case of a grounded fault, the algorithm first checks for different LG faults; if not concluded, the only remaining possibility is an LLG fault. Then a trained PNN is activated for LLG faults to identify the faulted phases. A PNN application for only LLG faults gives better overall accuracy and makes the algorithm suitable for real-time implementation. A brief description of PNNs followed by the overall flowchart is given below.

PNNs: a PNN is a supervised learning network that belongs to the general category of radial basis networks. Many classification problems utilize pattern recognition techniques that are based on the theory of Bayesian classification [22]. These techniques, realized by probabilistic model networks, require estimation of probability density function (PDF) and for an input x belonging to a category A. The PDF is given by

$$f_A(X) = \frac{1}{(2\pi)^{p/2}\sigma^p}\frac{1}{m}\sum_1^m \exp\left[-\frac{(X - X_{Ai})^T(X - X_{Ai})}{2\sigma^2}\right] \tag{3}$$

where i is the pattern number, m is the total number of training patterns, X_{Ai} is ith pattern from category A, σ is the smoothing parameter, and p is the dimensionality of measurement space. The smoothing parameter is fixed by the spread value in MATLAB simulation.

With enough training data, a PNN is guaranteed to converge and its fast learning makes it suitable for real-time applications, as in [23]. In the present application, the PNN is initially trained with several NETE patterns obtained from the simulation for different LLG faults. Patterns are generated by considering wide variations in FIA, R_f, and fault location. The PNN will have seven inputs and a single output, as shown in Figure 6a. The overall flowchart for the proposed scheme is shown in Figure 6b. The value of ε (single threshold) is set to be very small and should be ideally zero.

3. Simulation details and results

The classification procedure developed above was verified by simulation using the 400 KV line shown in Figure 1 with the parameters given in Table 2. The system was simulated in MATLAB/SIMULINK with a distributed parameter model (Bergeron's model) for the transmission lines, so that the fault signals exhibited the high-frequency transient components generated. Wavelet decomposition was done using bior2.2 as the mother wavelet because of its effectiveness in processing power system transients [24]. A total of 14,040 different fault cases were considered for simulation by varying fault type, fault location, FIA, and R_f, as shown in Table 3, to verify the performance of the proposed algorithm with a practical value of 0.02 for ε. The transient energy patterns obtained for different faults are shown in polar scatter plots to justify the validity of the proposed algorithm.

Table 2. 400 KV Transmission line parameters.

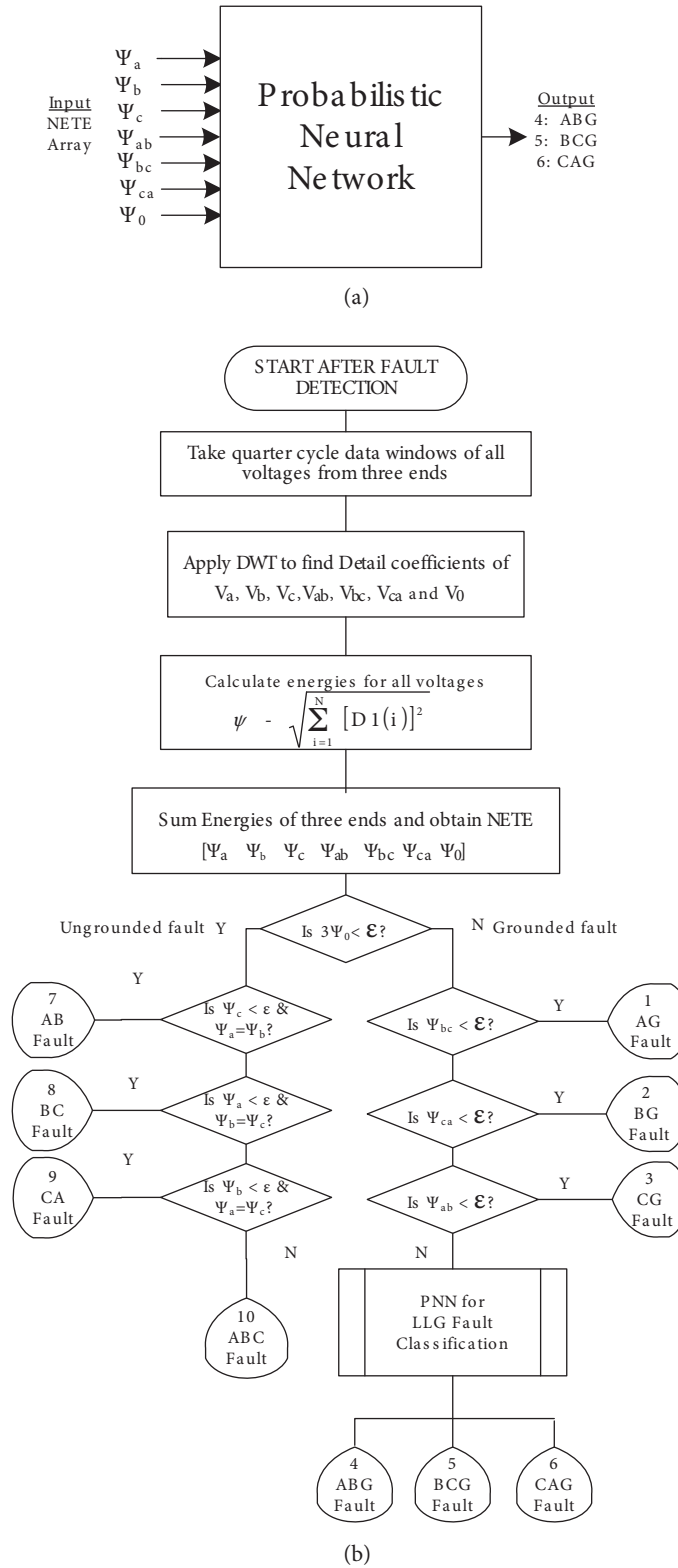| $R_1 = 0.029792\ \Omega/km$	$L_1 = 1.05678$ mH/km	$C_1 = 11.04137$ nF/km
$R_0 = 0.16192\ \Omega/km$	$L_0 = 3.947042$ mH/km	$C_0 = 7.130141$ nF/km

(a)

(b)

Figure 6. a) Inputs and outputs for the PNN. b) Overall flowchart for the proposed algorithm.

Table 3. Fault conditions considered.

Condition	Range
Fault type	AG, BG, CG, AB, BC, CA, ABG, BCG, CAG, ABC
Fault resistance	0 Ω, 50 Ω, 100 Ω
Fault inception angle	0° to 350° in steps of 10°
Fault location	Every 10 KM in each section
Total number of cases	14,040 (1404 for each fault type)

The performance of the proposed technique for LG faults was assessed by simulating 4212 faults at different locations. Figures 7a and 7b show the variation of transient energy with FIA on phase and line voltages, respectively, for AG faults (1404 cases). Note that Ψ_b and Ψ_{ab} patterns are not visible in these plots as they lie beneath Ψ_c and Ψ_{ca}, respectively. Although the energy values of phase voltages for both faulted (Ψ_a) and unfaulted (Ψ_b and Ψ_c) lines are nearly overlapping, the values of line voltages clearly indicate the faulted phase; i.e. for all AG faults, the value of Ψ_{bc} approaches zero. The present procedure had an accuracy rate of 100% in classifying LG faults.
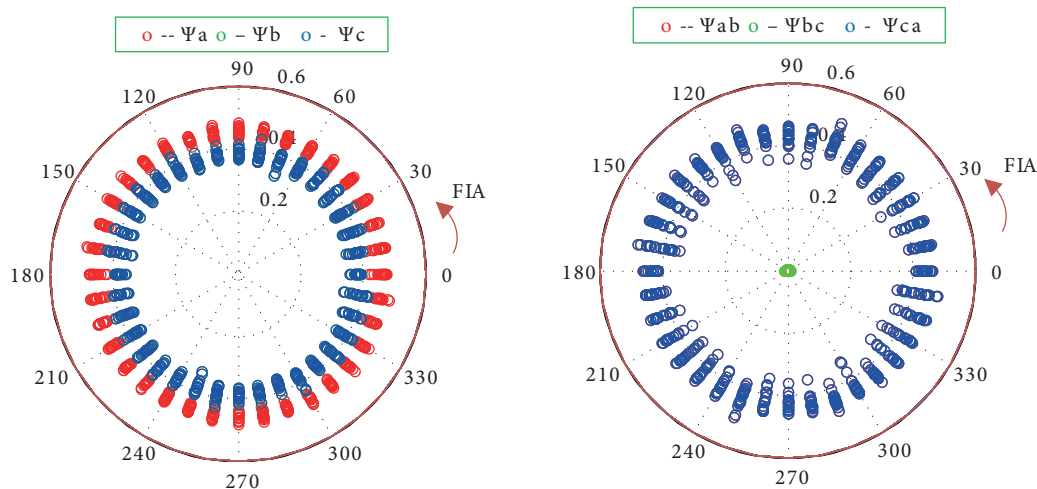
Figure 7. Energy patterns for AG faults a) phase b) line.

In LLG faults, the transients generated clearly brought out the typical patterns that make classification difficult. Figures 8a and 8b show the variation of energy on phase voltages for ABG faults with two different R_fs (0 and 100 Ω). The unfaulted phase energy (Ψ_c) was more than the faulted phase energy for a range of inception angles and this range was large, with an increase in R_f. Similar patterns were obtained for BCG and CAG faults as well. The symmetry of patterns in the polar plots shows that consideration of FIA variation from 0 to 180° is very much necessary while developing transient-based classification algorithms.

Regarding performance levels, the PNN was activated for all LLG faults without fail, and the classification accuracy with the trained PNN was very high (99.59%). The results of the 4212 cases simulated validate the application of PNN for classifying only LLG faults.

In the LL faults, the present technique classified all faults except 2 (out of 4212 cases) correctly by using the energy values of the phase voltages. Figure 9a shows the variation in energy of phase voltages for all phase A-to-phase B (AB) faults simulated (Ψ_a patterns not visible). Clearly, the unfaulted phase always exhibited
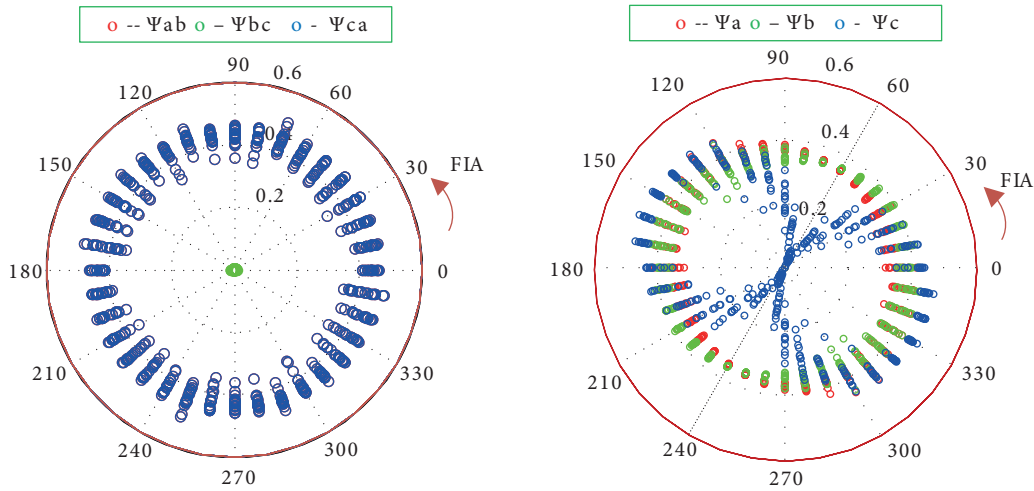
Figure 8. Energy patterns on phase voltages for ABG faults a) $R_f = 0 \ \Omega$, b) $R_f = 100 \ \Omega$.

a value of energy (Ψ_c) close to zero. The normalized energy on faulted phase voltage signals (Ψ_a and Ψ_b) remained fairly constant at 0.353. A similar pattern was obtained for BC and CA faults as well.
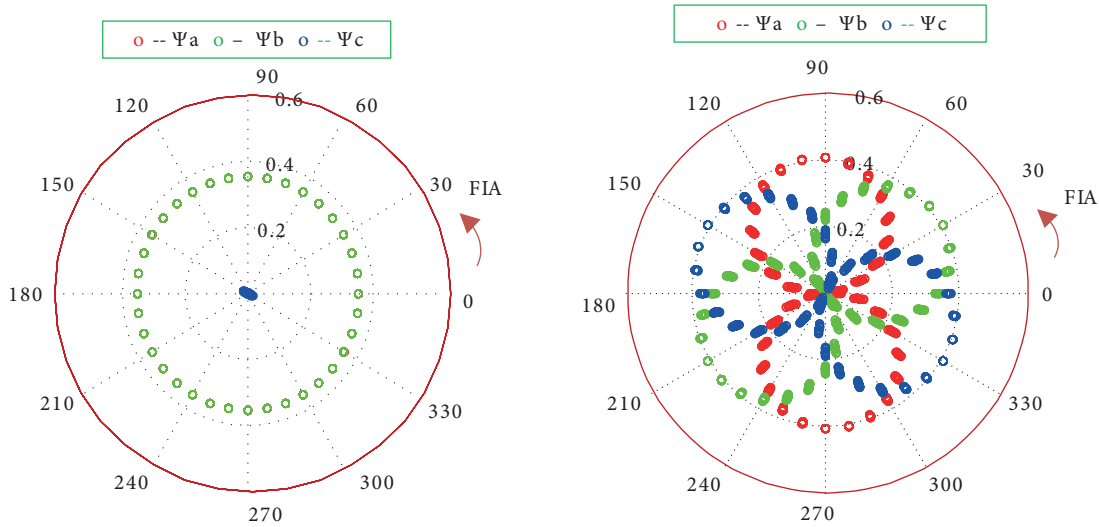

Figure 9. Energy patterns on phase voltages a) AB faults, b) ABC faults.

All the symmetrical three-phase faults (ABC faults) simulated were classified by the present method with 100% accuracy. Figure 9b shows the typical transient patterns developed on phase voltages for three-phase faults. The NETE magnitudes of different voltage signals varied widely with respect to FIA and in no case did the NETE meet the pattern of any LL fault.

The overall accuracy of performance with the proposed hybrid classifier was very high. Particularly, its ability to classify more frequent LG faults with 100% accuracy is an attractive feature. The results of the simulation show that the technique is quite insensitive to fault location, R_f, and FIA, which is a definite advantage over conventional phasor-based methods. Moreover, the classification of LLG faults using a PNN overcomes the major drawback of many existing transient-based methods in classifying LLG faults. Table 4 gives the complete simulation results for all 14,040 faults considered, with only 17 misclassifications in total. A

performance comparison with three recently reported methods [7,17,25] in Table 5 reveals the improvement in accuracy achieved by the proposed technique.

Table 4. Classification results.

Given fault type (All 1404 cases)↓	Fault classification result									
	1 AG	2 BG	3 CG	4 ABG	5 BCG	6 CAG	7 AB	8 BC	9 CA	10 ABC
AG	1404	0	0	0	0	0	0	0	0	0
BG	0	1404	0	0	0	0	0	0	0	0
CG	0	0	1404	0	0	0	0	0	0	0
ABG	0	0	0	1400	0	2	2	0	0	0
BCG	0	0	0	1	1397	4	0	2	0	0
CAG	0	0	0	2	2	1398	0	0	2	0
AB	0	0	0	0	0	0	1404	0	0	0
BC	0	0	0	0	0	2	0	1402	0	0
CA	0	0	0	0	0	0	0	0	1404	0
ABC	0	0	0	0	0	0	0	0	0	1404

Table 5. Accuracy of classification.

Sl. no.	Fault type	Number of cases cases	Accuracy %	Accuracy % reported by [7]	Accuracy % reported by [17]	Accuracy % reported by [25]
1	LG	4212	100	100	95.3	99.72
2	LL	4212	99.95	100	99.3	100
3	LLL	1404	100	100	99.7	100
4	LLG	4212	99.59	90.61	96.8	97.50
Overall		14040	99.88	99.53*	97.77	99.17

*Based on the probability of occurrence of different types of faults.

4. Conclusions

This paper presented a new voltage transient-based fault classification technique for three terminal lines that requires communication from the three ends for processing fault-induced voltage transients. An analysis of transient patterns revealed the influence of FIA and R_f, and that FIA variation from 0 to $180°$ needs to be considered while designing transient-based schemes. Based on investigations into fault transient patterns, a hybrid algorithm was developed by including a PNN to resolve the misleading transient pattern problem with LLG faults. The deterministic procedure for LG, LL, and LLL faults is very effective, with near 100% accuracy, whereas the PNN solution for LLG faults was 99.59% accurate. The proposed method copes well with the adverse influence of FIA and R_f. The exhaustive simulation results presented indicate the accuracy of the scheme with all types of faults, and its speed is evident from the use of only a quarter-cycle of fault voltage signals for processing. The method is simple, as it requires only voltage measurements, single threshold setting, and first-level wavelet decomposition.

In practical implementation, the bandwidth of the transducers, communication requirements, and processor speed play a significant role. Optical PTs having a wide bandwidth and fiber-optic communication systems

are needed in this scheme. Scope for further work includes hardware implementation and development of a noise-tolerant communication-free technique.

References

[1] Carter AM, Aggarwal RK, Johns AT, Bo ZQ. Computer-aided design of a new non-unit protection scheme for EHV teed circuits. IEE Proc-C 1996; 143: 140-150.

[2] Bhalja B, Maheswari RP. New differential protection scheme for tapped transmission line. IEE Proc-C 2008; 2: 271-279.

[3] Zhang N, Kezunovic M. Transmission line boundary protection using wavelet transform and neural network. IEEE T Power Deliver 2007; 22: 859-869.

[4] Mahamedi M, Guo Zhu J. Fault classification and faulted phase selection based on the symmetrical components of reactive power for single-circuit transmission lines. IEEE T Power Deliver 2013; 28: 2326-2332.

[5] Dong X, Kong W, Cui T. Fault classification and faulted-phase selection based on the initial current travelling wave. IEEE T Power Deliver 2009; 24: 552-559.

[6] He Z, Fu L, Lin S, Bo Z. Fault detection and classification in ehv transmission line based on wavelet singular entropy. IEEE T Power Deliver 2010; 25: 2156-2163.

[7] Valsan SP, Swarup KS. Wavelet transform based digital protection for transmission lines. Int J Elec Power 2009; 3: 379-388.

[8] Youssef ASO. Combined fuzzy-logic wavelet-based fault classification technique for power system relaying. IEEE T Power Deliver 2004; 19: 582-589.

[9] Reddy MJ, Mohanta DK. A wavelet-fuzzy combined approach for classification and location of transmission line faults. Int J Elec Power 2007; 29: 669-678.

[10] Vasilic S, Kezunovic M. Fuzzy ART neural network algorithm for classifying the power system faults. IEEE T Power Deliver 2005; 20: 1306-1314.

11 Silva KM, Souza BA, Brito NSD. Fault detection and classification in transmission lines based on wavelet transform and ANN. IEEE T Power Deliver 2006; 21: 2085-2063.

[11] Dash PK, Samantaray SR, Panda G. Fault classification and section identification of an advanced series-compensated transmission line using support vector machine. IEEE T Power Deliver 2007; 22: 67-73.

[12] Jiang JA, Chuang CL, Wang YC, Hung CH, Wang JY, Lee CH, Hsiao YT. A hybrid framework for fault detection, classification, and location-part i: concept, structure, and methodology. IEEE T Power Deliver 2011; 26: 1988-1998.

[13] Jamehbozorg A, Shahrtash SM. A decision-tree-based method for fault classification in single-circuit transmission lines. IEEE T Power Deliver 2010; 25: 2190-2196.

[14] Upendar J, Gupta CP, Singh GK. Statistical decision-tree based fault classification scheme for protection of power transmission lines. Int J Elec Power 2012; 36: 1-12.

[15] He Z, Lin S, Deng Y, Li X, Qian Q. A rough membership neural network approach for fault classification in transmission lines. Int J Elec 2014; 61: 429-439.

[16] Livani H, Evrensoglu CY. A fault classification and localization method for three-terminal circuits using machine learning. IEEE T Power Deliver 2013; 28: 2282-2290.

[17] Brahma SM. Distance relay with out-of-step blocking function using wavelet transform. IEEE T Power Deliver 2007; 22: 1360-1366.

[18] Chen W, Malik OP, Yin X, Chen D, Zhang Z. Study of wavelet-based ultra high speed directional transmission line protection. IEEE T Power Deliver 2003; 18: 1134-1139.

[19] Brahma SM, De Leon PL, Kavasseri RG. Investigating the option of removing the anti-aliasing filter from digital relays. IEEE T Power Deliver 2009; 24: 1864-1868.

[20] Osman AH, Malik OP. Transmission line distance protection based on wavelet transform. IEEE T Power Deliver 2004; 19: 515-523.

[21] Specht DF. Probabilistic neural networks. Neural Networks 1990; 3: 109-118.

[22] Perera N, Rajapakse AD. Recognition of fault transients using a probabilistic neural network classifier. IEEE T Power Deliver 2011; 26: 410-419.

[23] Shaik AG, Ramana Rao PV. A new wavelet based fault detection, classification and location in transmission lines. Int J Elec Power 2015; 64: 35-40.

[24] Mollanezhad Heydar-Abadi M, Akbari Foroud A. Accurate fault classification of transmission line using wavelet transform and probabilistic neural network. Iranian Journal of Electrical and Electronic Engineering 2013; 9: 177-188.

[25] Coteli R. A combined protective scheme for fault classification and identification of faulty section in series compensated transmission lines. Turk J Elec Eng & Comp Sci 2013; 21: 1842-1856.

[26] Guillen D, Paternin MRA, Zamora A, Ramirez JM, Idarraga G. Detection and classification of faults in transmission lines using the maximum wavelet singular value and Euclidean norm. IET Gener Transm Dis 2015; 9: 2294-2302.

[27] Yumurtaci M, Gokmen G, Kocaman C, Ergin S, Kilic O. Classification of short-circuit faults in high-voltage energy transmission line using energy of instantaneous active power components-based common vector approach. Turk J Elec Eng & Comp Sci 2016; 24: 1901-1915.